Natural Resources for Human Health
eISSN: 2583-1194

Original Research

Received 24 July 2026
Revised 19 Aug 2026
Accepted 03 Sep 2026

Natural Resources for Human Health 2026, Vol. 6 (21s): 695–711

KEYWORDS:
Emotion Recognition, Machine Learning, Segmentation, Optimisation, Multi-channel EEG signals

Multi-Channel EEG Signal Processing in Emotion Recognition by Segmentation and Optimisation Using Machine Learning Algorithms

*[1]Dr. A. Sampath, [2]Mrs. K.M. Swarna Devi

[1]Department of Electrical and Electronics Engineering, Kongunadu College of Engineering and Technology, Tiruchirapalli.
E-mail: sampath461@gmail.com
[2]Department of Computer Science and Engineering, Kongunadu College of Engineering and Technology, Tiruchirapalli, India
E-mail: swarnadevikm@gmail.com
Corresponding Author *1Dr. A. Sampath
E-mail: sampath461@gmail.com

ABSTRACT: Human decision-making, planning, thinking, and other mental processes are all greatly influenced by emotions, which are an essential part of everyday life. They are therefore regarded as an important component of human interactions. Human emotions are recognised from different sources, combining speech, body language, facial expressions and behaviour (position and gesture). The brain's electroencephalogram (EEG) impulses provide us with a more varied understanding of emotional states that people might not be able to articulate. This research proposes novel technique in emotion recognition based on segmentation with optimisation using multi-channel based EEG with Machine Learning (ML) model. Emotion recognition utilizingmulti-channel EEG signals with ML involve analyzing brain activity captured by two EEG channels to identify emotional states, leveraging ML algorithms for classification. EEG signals collects the inputs are processed for the noise removal process. Then this signal has been segmented utilizing multi-channel graph cut attention convolutional neural networks. From this segmented the EEG signal has been pipelined based on discrete residual transform with artificial grey wolf swarm optimization. The experimental Analysis was done in terms of finding accuracy, mean average precision, recall, F-1 score, AUC. The proposed model achieved detection accuracy. is 97%, mean average precision is 95 %, recall is 93%, F-1 score is 91%, AUC is 90%.

1. INTRODUCTION:

Emotional states impact this capacity to respond rationally in situations involving perception, human intellect, and decision-making as they are closely associated with various human emotions, thoughts, and behaviours. Therefore, brain–computer interface (BCI) systems have emerged as a valuable part of the research for therapeutic applications and human social interactions through the recognition of emotions from emotional signals [1]. Psychological diseases like autism spectrum disorder (ASD), attention deficit hyperactivity disorder (ADHD), anxiety disorder are being studied using physiological signals, taking into account the natural components of emotions. EEG-based emotion identification systems have gained popularity among cognitive scientists as a study topic in recent years. The major challenges in developing EEG signals are utilized by an emotion detection system for precise categorization and efficient feature extraction. EEG signals are

unpredictable, non-stationary, non-linear, obscured by several types of noise [2]. Therefore, managing and deriving significant information from EEG signals is essential to successful construction of an emotion identification system. EEG signals are quantified using extracted features, which are subsequently utilised as classifier qualities. In intelligent emotion identification methods, a range of features have been retrieved from EEG signals in, joint time-frequency section, time section and frequency domain. Signals in particular frequency bands can be broken down by the wavelet transform with the least amount of time-resolution loss. The signal acquisition stage, which forms the first component of a BCI system, captures and it records brain activity signals and forwards them to initial stage for reducing noise and improving quality. There are two categories of brain signal acquisition techniques: invasive and non-invasive. Electrodes are neurosurgically positioned within or on top of the user's brain in invasive techniques. Non-invasive technology uses external sensors to monitor brain activity [3]. Following preprocessing, the many characteristics of the significant signal—such as the signal's association with the user's intention—are separated from extraneous information and displayed in a manner that enables their conversion into output instructions.In addition to reducing the amount of data that can be sent to the translation algorithm, this component produces selective features for the enhanced signal and transforms characters into the pertinent instructions that the external device needs to finish the task (such as instructions that fulfil the user's intent). The translation algorithm uses the instructions it has learnt to guide and control the output device. Despite its limited spatial resolution and the need for multiple electrodes placed across different regions of the head, EEG provides adequate temporal resolution, allowing researchers to investigate phase changes in response to emotional stimuli [4]. EEG is a more popular technique for examining how the brain reacts to emotional stimuli since it is quick, easy, and affordable. Numerous attempts aremade to examine the use of ML techniques, including Deep Neural Networks (DNN), Logistic Regression (LR), k-nearest Neighbours (KNN), Support Vector Machines (SVM)Dynamic Graph Convolutional Neural Networks (DGCNN), in the examination of feelings in EEG signals; nevertheless, numerous obstacles still exist. To achieve robust and accurate categorisation, challenges include inter-individual variability, intrinsic noise in EEG recordings, overlap of brain activation patterns between distinct emotions [5]. Application of ML as well as DL methods, which have become a viable strategy for improving emotion recognition from EEG signals, forms theoretical foundation of this study. While KNN categorises emotions based on how closely EEG patterns resemble those of labelled samples, LR predicts the likelihood of an emotional state as a function of EEG features. Deep learning (DL) techniques have drawn a lot of interest in field of EEG-based emotion identification in an effort to overcome these constraints. DNNs, a subset of DL methods, can independently generate hierarchical representations from unprocessed EEG signals. DNNs outperform conventional ML models in emotion classification tasks by extracting more abstract and significant characteristics from the EEG data by stacking multiple layers of artificial neurones [6]. Novelty of this research: to provide a new segmentation-based emotion recognition method that optimises the use of dual channel EEG with a ML model. Here, the EEG signal is gathered as input and processed for normalisation and noise reduction. Dual channel graph cut attention convolutional neural networks were then used to segregate this signal. The EEG input has been segmented and then pipelined using artificial grey wolf swarm optimisation and discrete residual transform. To solve two important problems in crosssession EEG emotion identification, provide a transfer metric learning approach. In particular, domain alignment extracts domain-invariant features to address cross-session variations by aligning the feature distributions of the two sessions, while graph-based metric learning captures discriminative features to handle cross-trial differences by connecting the EEG samples through different trials that shares equal emotional state. The efficacy of these two modules is clearly shown by the comprehensive testing findings.

2. LITERATURE SURVEY:

Field of EEG research is expanding its applications into other subfields. As demonstrated in [7], EEG signals are frequently utilised to identify stress, and there appears to be a high link between stress and EEG signals. Work [8] employed the Hilbert-Huang Transform (HHT) for signal cleaning and artifact removal. HHT is a technique for analyzing time-frequency that employs empirical mode decomposition to fetch intrinsic mode functions (IMFs), which provide well-defined Hilbert transforms of the analyzed signals. The IMF provides instantaneous frequencies as a function of time using the Hilbert transformation. With an accuracy of 89%, their application of hierarchical SVM produced far better results than a linear SVM. Even when evaluating traditional ML methods, it is required to consider a number of different parameters. Their findings motivated us to investigate and include cross-validation into this trials using a grid search. The author [9] used DL with back propagation and the Fast Fourier Transform to figure out the optimal technique to smooth stress, although they only got a 75% accuracy rate. EEG signals can be utilized to control robotic arms in motor imagery-based applications [10].

The ability of BCI to recognise and differentiate between people's brain waves while they are undertaking various tasks was described in Work [11]. An automative EPOC served as the foundation for its implementation, which tested the classifier "SVM's" ability to differentiate between two main training tasks: moving the left hand and the right foot, as well as four more combinations of the two movements plus sounds, such as nodding or moving the right foot and left hand. Additionally, it has been noted that faces can be seen even when none are present, indicating that EEG can be used to detect optical illusions [12] and identify the brain regions that are more active in the early stages of visual processing (before one can think unconsciously). It is discovered that the perceptual signatures of P100 and N170 are significantly more significant than the rest. DL has been applied to motor imagery, as demonstrated in [13], which put out the high-level objective of identifying reliable representations from EEG data that would be immune to intra- and inter-subject variations as well as to intrinsic noise present in EEG data gathering. Work [14] first used LSTM to extract characteristics through EEG signals close to dense layer and then utilized a DL approach to identify emotions from unprocessed EEG data. The extracted features were subsequently classified in a sequence according to low/high arousal, valence, and preference. This method was confirmed using the DEAP dataset, gets average accuracies of 85.65%, 85.45%, and 87.99% for the liking, valence, and arousal classes, respectively. Based on 14-channel recordings, Author [15] acquired EEG data from 21 healthy participants using specialized sensors that measured electrical brain activity. During the recordings, participants viewed photographs representing four emotional triggers: joyful, relaxed, sorrowful, and fearful. A statistical approach was employed during feature extraction to obtain relevant features from different frequency bands. Work [16] subsequently with the use of DNN to recognize emotions from human through EEG signals obtained through this DEAP dataset. Using same dataset, proposed approach was contrasted with most advanced emotion detection algorithms. The work demonstrated how DNNs may be used to do EEG-based emotion identification, especially when dealing with a large number of training datasets. A novel methodology for automatically identifying emotion from EEG signals was reported by the author [17]. The EEG signal was recorded by these researchers using 128 channels. Furthermore, correlation-based feature selection (CFS) was helps to identify the active EEG channels among 32 participants, revealing the five channels are T3, F3, Fp1, O2 and lastly Fp2 had a significant influence on recognition of emotion. The study subsequently applied a genetic algorithm (GA) to minimize the dimensionality of the vector of feature and used a t-test to validate the accuracy of the features of selected. Lastly, classification was done using the Bayesian, RF, KNN, and multilayer perceptron classifiers. Work [18] used EEG waves to identify four emotions of surprise, happiness, sadness, tranquilly. The EEG signal was recorded using eight subjects. For the classification portion, these researchers employed four classifiers RF, SVM, LDA, C4.5. They found that C4.5 classifier performs better at identifying emotion. To identify emotion, the author [19] employed a fuzzy parallel cascade (FPC) model. These researchers used 15 volunteers and a musical cue for their investigation. Additionally, they contrasted recurrent neural networks (RNN) with their suggested model. Last but not least, these researchers' mean squared error (MSE) for classifying the two valence and arousal classes is approximately 0.089, which is less than that of other models. DNNs were employed in study [20] to identify emotion from EEG waves. Twelve persons participated in their experiment. They suggested using six convolutional layers in their network architecture. Furthermore, these researchers found that CNN performs better in emotion recognition than comparison approaches after comparing their suggested method with SVM. Two groups of emotions were automatically classified by the author [21] using EEG signals. These researchers' suggested approach made advantage of parallel RNNs. According to their suggested method, final announced accuracy for valence- and arousal-class categorisation was 93.64% and 93.26%, respectively.

3. PROPOSED EMOTION RECOGNITION BASED ON SEGMENTATION WITH OPTIMISATION USING MULTI-CHANNEL BASED EEG WITH MACHINE LEARNING MODEL

The input multichannel EEGs are considered as a whole in the suggested computing paradigm in order to feed into method that is intended for direct emotion detection. $x \in RK \times N$ represents the input multichannel EEGs, where K is number of electrodes placed onbrain to record EEG and N is longest timestamp that can be recorded. Usually it uses a sliding window of length N to create fixed-length EEG segments for lengthy time series. The suggested pattern recognition model transforms a matrix input x transforms into an output vector $y \in RC$, where each $yi \in \{0,1\}$ represents the likelihood that the input sample corresponds to emotional class Ci. Dataset overview: SEED Dataset: As seen in Table 1, the SEED dataset was essential in eliciting participants' emotional reactions when they watched short videos. These Chinese films were all accompanied by a musical composition to heighten emotional impact. Experiment's design was to replicate a naturalistic environment in order to elicit notable physiological responses. Fifteen clips, each lasting four minutes on average, were used

in each session. Each of the three emotional categories—happiness, sadness, and neutrality—is represented by five different movie clips in the dataset. A five-second teaser of each clip was shown to participants, who then had a reflection phase of 45-second and a rest interval of 15-second during the structured session. Self-report questionnaires were used to gauge the respondents' emotional states. Chinese students who claimed to have normal vision and hearing made up the group. With a minimum of one week separating each session, each subject underwent the experimental process three times Following the 10–20 system, the EEG data was captured with a sixty-two-channel electrode, sampled at 1000 Hz, filtered within the range of 0.5 to 70 Hz, and then reduced to 200 Hz for analysis. DEAP Dataset. One essential resource for emotion identification using EEG waves is the DEAP dataset. It includes recordings made by 32 subjects who watched music videos under observation (Table 1). With the help of a 40-channel setup with continuous reference, the brain activity of each participant was captured throughout 40 video sessions. The data was first collected at 512 Hz and then processed to 118 Hz. During the study, participants viewed a series of video segments, each linked to four emotional aspects: arousal, valence, dominance, and preference/displeasure. Participants' personal reactions to each stimulus were gathered through self-report questionnaires addressing these four emotional aspects. Utilizing DEAP dataset, nine different emotional states were identified in many dimensions: happiness, calm, fear, excitement, indifference, and sadness.

Table 1: Structure of the database.

Dataset	Name of the array	Size of the array	Contents in the array
SEED dataset	EEG data	18x62x48000	Videos/trails x channels x samples
	Labels	15 x 3	Videos/trails x labels
DEAP dataset	EEG data	40 x 40 x 8064	Videos/trails x channels x samples
	Labels	40 x 4	Videos/trails x labels

A. GAMEEMO Dataset

This research utilized the dataset of GAMEEMO, containing signals of EEG collected from 28 individuals. The EEG signals in this dataset have a total length of 38,252. The research included 28 participants who were aged 20 to 27 years. EEG signals were captured during gaming sessions on a computer using a portable and wearable 14-channel Emotiv EPOC+ EEG system. Every participant provided 20 minutes of EEG data collected while engaging in four emotionally different computer games, each lasting five minutes: dull, soothing, frightening, and funny. In contrast to traditional datasets mentioned in earlier research, this dataset employed video games as emotional triggers. The signals of EEG were gathered using a mobile 14-channel device featuring are AF3, AF4, F3, F4, F7, F8, FC5, FC6, O1, O2, P7, P8, T7, and T8 channels, featuring Wi-Fi enabling wireless communication during data collection. Both dimensional and discrete emotion models were taken into account when creating the dataset. Four games in total—designated G1, G2, G3, and G4—were played in the study in order to record emotions. Positive emotions are expressed by G2 and G4, whilst negative emotions are expressed by G1 and G3 in the discrete emotion model structure. G1 stands for LANV, G2 for LAPV, G3 for HANV, and G4 for HAPV in the arousal-valence dimensional model. The GAMEEMO data set's specifics are explained in Table 2. These signals are sampled at 128 Hz frequency. The data collection includes both raw and preprocessed EEG recordings, while the accompanying report provides detailed technical information about the dataset.

Table 2. The stimuli utilized in the GAMEEMO dataset.

Game symbol	Stimuli type	Dimensional model	Discrete model
G1	Boring	LANV zone	Negative emotion
G2	Calm	LAPV zone	Positive emotion

G2	Horror	HANV zone	Negative emotion
G4	Funny	HAPV zone	Positive emotion

Channel selection: The 32 channel data in the dataset used to test the suggested approach is accessible in 63 seconds at a frequency of 128 Hz. Therefore, a vast amount of data must be handled for every individual. This leads to two issues: first, the massive volume of data necessitates a large quantity of storage memory, second, processing process takes a lengthy time. These two drawbacks led us to choose to decrease the data set, even if the classification accuracy remained constant. Discovered that the 7.5-second data set used in this study is suitable for this suggested algorithm's easy feature extraction. Although this significantly reduces the data processing load, further reduction can be achieved by selecting specific channels and processing only their associated data. The algorithm's feature extraction time and channel usage should be kept to a minimum if it is designed for real-time applications. The degree of comfort experienced by the person using the device is also impacted by the number of electrodes employed. Therefore, primary goal is to suggest an algorithm that operates in real-time applications with sufficient precision. Various techniques, mostly based on heuristic optimisation algorithms or trial and error, have been documented to identify the most efficient pathways. Based on results of reported methodologies, this study compares two sets of channels. Three channels—P7, P3, and PZ—are included in one group, while seven channels—P7, P3, PZ, PO3, O1, CP2, and C4—are included in the other. As a result, there is significantly less data.

4. METHODOLOGY:

The electrical activity of brain over time is reflected in EEG data. They include details on how the human body as a whole is controlled. Provide a novel proposed approach to fetch features through EEG sources according to the subject's brain condition. The proposed approach initially identified high-resolution EEG signal epochs and analyzed brain activity variations across the selected electrodes. It then identified the EEG channels exhibiting the most pronounced changes during different emotional states. Features were extracted from these pertinent electrodes, which vary from person to person according on their mental state. Alpha, beta, delta, gamma are four EEG rhythms from which a distinct set of electrodes is selected for each person. The attributes needed to identify and categorise nine emotions were computed using these sources. Figure 1 displays the suggested method's flow diagram.

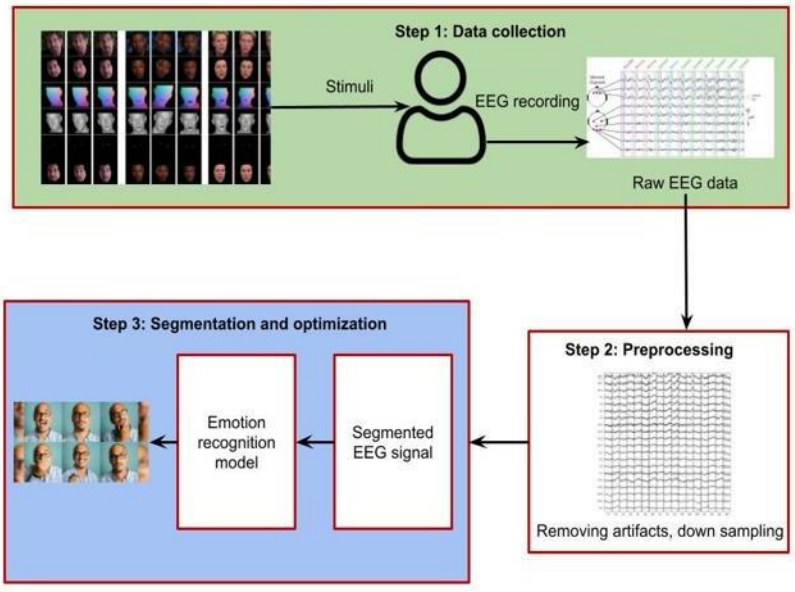


Fig-1 proposed emotion recognition based on segmentation with optimisation

A. Pre-processing

i. Filtering

Preprocessing raw data is essential in field of EEG to enhance quality of EEG readings due to various forms of background noise. EEG signals primarily consist of four major delta frequency bands of (0–4 Hz), theta of (4–8 Hz), alpha of (8–13 Hz), and beta of (13–30 Hz), with the frequency range extending up to 50 Hz. These rhythms give valuable insights into fundamental patterns of brain activity and are widely analyzed in medical applications. The proposed study uses a Hanning window and a unique Dual Tree complex wavelet method to derive characteristics from the data. These qualities are then classified as neutral, bad, or positive using the Valence Arousal Two-Dimensional Approach. Ratings above the mean are classified as high arousal/valence (positive, 1), whereas as elevated arousal/valence (positive, 1), while scores beneath the median are classified as reduced arousal/valence (negative, 1). Scores at or beneath the median are regarded as neutral arousal/valence (0, 0). A binary categorisation assignment was created in order to calculate ability to recognise emotions. To enhance quality of EEG signals, raw data must be pre-processed. Software-based methods are employed to semi-automatically remove EOG and other artifacts through EEG recordings with the help of Independent Component Analysis (ICA), particularly the FastICA algorithm. Filtering is utilized as first stage in signal processing, then signal is broken down into smaller bands by eqn (1)

$$y(t) = \int_{-\infty}^{\infty} z(\tau) \cdot f(t-\tau) d\tau \quad (1)$$

Restructuring and Rearrangement: The acquired data for the emotion recognition assignment was first organized as video × channel × data = 40 × 40 × 8064, relating to 40 videos, 40 channels, and 8064 data points. After retaining the original 60-second data segments, the data was reshaped to video × channel × data = 40 × 32 × 7680. The dimensions were then rearranged through permutation to obtain channel × data × video = 32 × 7680 × 40. Decomposition- Human labour activity has a complete impact on brain waves. Consequently, it is possible to derive the circumstances and mental states from the EEG data. Different activities and mental states are incorporated within the various sub-bands. For example, deep sleep and unconsciousness are associated with delta sub-band, which is associated with tranquil or calming activities. Imagination, sleepiness, eye closure, other low-level excitation are associated with theta and alpha sub-bands. Beta sub-band signal incorporates medium-level excitements, such as thinking, anxiety, tension. Finally, hyperactivity-related behaviours like attentiveness, agitation, object matching, sensory processing are impacted by gamma sub-band signals. In this section of this work, utilizedDWT to break down EEG data into five sub-bands. Later, disregarded the delta and theta sub-bands for emotion identification since they were linked to low-level, relaxing brain activity. The first participant's (p1) The original EEG signal is examined using the alpha, beta, and gamma sub-band signals from channel Fp1 for the first video (v1).

5. MULTI-CHANNEL GRAPH CUT ATTENTION CONVOLUTIONAL NEURAL NETWORKS (MCGCACNN)

The GAT is capable of representing the connections between any nodes in a graph that includes k nodes, labeled as v1,v2,…,vk. In this context, vi∈Rm denotes the learned representation of the i-th EEG channel at a given timestamp, derived through a 1-D CNN. These connections are established utilizing the subsequent equation (2):

$$h_i = \sigma(\sum_{j=1}^{L} \alpha_{ij} v_j) \quad (2)$$

Where hi represents the updated depiction of channel i influenced by data from its neighboring nodes. The function σ, similar to the sigmoid activation function, nonlinear activation function is denoted. The attention coefficient αij measures the extent of correlation between node i and its neighboring node j, as described in Equation (3).

$$\epsilon_{ij} = \text{ReLU}\left(a^T \cdot (v_i \oplus v_j)\right)$$

$$_{ij}\alpha \quad \frac{\exp(e_{ij})}{\sum_{l=1}^{L} \exp(e_{il})} \quad (3)$$

where a ∈ R2m indicates the weight vector of the attention mechanism, ReLU refers to the nonlinear activation function, and ⊕ symbolizes the concatenation of the representations from both nodes. Express all characteristics, both labeled and

unlabeled, as X = [X1,..., Xn]. Graph information serves as explicit regularization based on the premise that closely connected nodes are more likely to share the same label, as shown in Equation (4).

$$\mathcal{L}(X, Y_L) = \mathcal{L}_{\text{label}}(X_L, Y_L) + \lambda \mathcal{L}_G(X) \quad (4)$$

where LG is graph-based regularisation, such as LG = P (i,j)∈E kf(Xi) − f(Xj)k 2, which is also known as graph Laplacian regularisation, and Llabel = P i∈L l(Yi, f(Xi)) is a common supervised loss utilized across different loss functions l. Earlier approaches were non-parametric and utilize it as a lookup table to explore all f. Considering the features X and the graph A, zic represents the predicted probability that the label at node i ∈ [n] is c ∈ [dy]. Data A ∈ {0, 1} n×n represents the adjacency matrix of graph G, while X ∈ R n×dx includes dx features for every node listed in each row. In a typical GNN, the forward pass switches between a single-layer perceptron and a propagation layer. Let t represent the layer index as per equation (5).

$$\tilde{H}^{(t)} = PH^{(t)} \quad (5)$$

The random-walk operation can be represented as H~i(t)=|N(i)|1∑j∈N(i)Hj(t), derived from P=D−1A. In this setting, N(i) represents the neighborhood of node i, whereas D=diag(A1) denotes the degree matrix. This simple local averaging technique is often employed in consensus-based and random-walk-based approaches. For the graph-convolution (GC) filtering projections Zk∈RNwh×ck, where k=1,2,3, these projections are merged to create Z=[Z1,Z2,Z3]=[z1,…,zNwh]T∈RNwh×d, with zi∈Rd denoting the multi-scale node features and d=∑kck. Subsequently, Z is reorganized into the tensor Z∈RN×w×h×d to serve as the input for Fgcm. In the end, a function FgGAP is developed to perform group global average pooling (gGAP), as described in Equation (6).

$$\boldsymbol{u} = \mathcal{F}_{gGAP}(\boldsymbol{Z}) = \frac{1}{Nwh} \sum_{n,i,j} \boldsymbol{Z}(n, i, j, z) \quad (6)$$

It encodes globally informative group-wise contextual information into a representation of multi-scale semantic saliency, generating a global statistical feature u∈Rd. Subsequently, u is correlated with Z to generate a set of attention maps that effectively capture intra-saliency relationships, as defined in Equation (7).

$$\boldsymbol{M}_{\text{att}} = \boldsymbol{u} \otimes \boldsymbol{Z} \quad \textbf{(7)}$$

where ⊗ represents the correlation operator and Matt ∈ R N×w×h. Next, rescale Matt's values to [0, 1] using the sigmoid function σ as eqn (8)

$$\boldsymbol{W} = \sigma(\boldsymbol{M}_{\text{att}}) \quad (8)$$

Though certain noisy non-co-salient foregrounds are emphasised, note how Matt finds intrasaliency that maintains spatial consistency. This problem can be mitigated by further refining the attention maps using an attention graph clustering technique, which can more effectively distinguish common objects from prominent foregrounds. The model's word embedding matrix W(0)∈Rdx×dh is optimized according to Equation (9).

$$H^{(1)} = \text{ReLU}(XW^{(0)}) \quad (9)$$

This is followed by several attention-driven propagation layers, each characterized by β(t)∈R, as specified in Equation (10).

$$\text{H}^{(\text{t+1})} = \text{P}^{(\text{t})}\text{H}^{(\text{t})} \quad (10)$$

where the output row-vector of node I equals zero for absent edges, and the propagation matrix P(t) ∈ R n×n is likewise dependent on input states H(t) as outlined in equation (11).

$$H_i^{(t+1)} = \sum_{j \in N(i) \cup \{i\}} P_{ij}^{(t)} H_j^{(t)} \quad (11)$$

with $P_i^{(t)} = \text{softmax}\left([\beta^{(t)} \cos(H_i^{(t)}, H_j^{(t)})]_{j \in N(i) \cup \{i\}}\right)$ and $\cos(x, y) = x^T y / \| x \| \| y \|$ and an integer rl. The number of propagation layers is represented here. Notably, the proposed propagation mechanism is dynamic, varying across layers according to different β(t) values and hidden states. It also learns to assign greater importance to more relevant neighboring a

higher weight, demonstrating its adaptability. To make sure that the node's hidden states and features are preserved during the propagation process, include a self-loop. Weight of output layer is W(1) ∈ R dh×dy by eqn (12)

$$Z = f(X, A) = \text{softmax}(H^{(\ell+1)}W^{(1)}) \tag{12}$$

In (13), a cross entropy loss is used to train weights W(0), W(1), β (t). Focus that node j is giving to node i is

$$P_{ij}^{(t)} = (1/C)e^{\beta^{(t)}\cos(H_i^{(t)},H_j^{(t)})}$$

$$\text{with } C = \sum_{i\in N(i)\cup(i)} e^{\beta^{(t)}\cos(H_i^{(n)},H_j^{(n)}),} \tag{13}$$

This, as determined by cosine of angle between respective hidden states, expresses how important j is to i.

6. DISCRETE RESIDUAL TRANSFORM WITH ARTIFICIAL GREY WOLF SWARM OPTIMIZATION (DRTAGWSO)

The block's output is superimposed on the input, which is X, and a shortcut is inserted after X. As a result, the block's output is F(X)+X, and F(X) is the network weight parameter that must be learnt. The skip connection in the identity mapping is a key component of the architecture. It directly adds the output of the previous layer to the output of the subsequent layer without introducing any additional learnable parameters. The residual blocks, which are the fundamental building blocks of deep ResNet and are defined as follows (14), are utilised throughout the network in the suggested model.

$$\mathrm{Y} = \mathrm{F}(\mathrm{X}, \{\mathrm{W}_i\}) + \mathrm{X} \tag{14}$$

X and Y stand for input and output vectors of specified layers. The residual mapping to be learnt is represented by the function F(X, {Wi }). The dimensions of X and F in Eq. (3) should be the same. The output vector from the previous layer is sent into the softmax function in the fully linked layer. The probability of estimated outcomes for the softmax function's output are produced using the formula below (15):

$$P(y = 1 \mid x, w, b) = \frac{\exp(w \cdot x + b)}{1 + \exp(w \cdot x + b)}$$

$$P(y = 0 \mid x, w, b) = \frac{1}{1+\exp(w \cdot x+b)} \tag{15}$$

where w stands for the weight parameter, b for a bias term, x for a feature vector, and y for the target class. The binary cross-entropy between estimates and targets is determined by this study using a binary cross-entropy function as the loss function. It is provided by eqn (16):

$$BCEL = -\frac{1}{N_0}\sum_{i=1}^{N0} [t_i \log(p_i) + (1 - t_i)\log(1 - p_i)] \tag{16}$$

In {0, 1}, where 0 is a normal control and 1 denotes a patient with schizophrenia, N0 denotes total number of training samples, pi denotes estimated result of each sample, and ti denotes the target class. The widely used Discrete Wavelet Transform (DWT) technique was employed for signal analysis. DWT is particularly appropriate for examining non-linear and non-stationary signals. across different frequencies and resolutions. It provides information about signal characteristics in both the time and frequency domains. In EEG analysis, DWT decomposes the signal into multiple components using a single basis function known as the mother wavelet, as represented by Equation (17).

$$\psi(t) = \frac{1}{\sqrt{2}}\psi\left(\frac{t-y}{x}\right) \quad x, y \in S, x > 0 \tag{17}$$

where S represents the wavelet space and x and y denote the scaling and shifting parameters. The equation below demonstrates that the wavelet transform is expressed by equation (18).

$$F(x, y) = \frac{1}{\sqrt{x}}\int \psi\left(\frac{t-y}{x}\right) dt \tag{18}$$

Natural Resources for Human Health
eISSN: 2583-1194

Given that DWT, as expressed by Eq. (19) offers a very effective version, which is utilized in this study. The filtered EEG signal was decomposed using low-pass and high-pass filters via the DWT to achieve the signal representation in terms of approximation (A1) and detail (D1) coefficients at the first decomposition level.

$$F(t) = \sum_{k=-\infty}^{k=+\infty} D_{n,k}\phi(2^{-n}t - k) + \sum_{k=-\infty}^{k=+\infty} \sum_{k=-\infty}^{k=+\infty} 2^{\frac{-1}{2}} A_{j,k}\psi(2^{-j}t - k) \quad (19)$$

In this context, n signifies the level of decomposition, ψ stands for the scaling function, while Aj,k and Dn,k reflect the approximation and detail coefficients, respectively. Subsequently, the detail coefficients for each decomposition level and the approximation coefficients at the final level were calculated to extract the relevant features from the EEG signals. Performance is assessed as well as computed. DWT was generally not combined with various statistical variables simultaneously. Traditional statistical features may be insufficient for describing non-stationary and non-linear signals and could fail to accurately capture the complex traits of EEG data. For a discrete signal S(n) defined by mean μ and standard deviation σ, where n=1,2,…,N with N indicating the total number of samples, further descriptive characteristics are thus taken into account. Specifically, aspects concerning EEG signal strength, like root mean square (RMS), along with data distribution characteristics are analyzed to derive more insightful signal representations. Explaining the power and information distributions of EEG signals, including the logarithmic band power, average power, norm, is essential. The ML techniques used in this study make it simple and accurate to classify certain attributes. The Alpha wolf is regarded as the pack's wisest member because to its extensive experience in decision-making and pack management. Selecting a habitat as well as managing hunting mechanism are its main responsibilities. The β wolves, who are found at the second level of domination hierarchy, typically assist α wolf in carrying out tasks like hunting prey and managing the pack. Third level of the hierarchy of dominance is occupied by the δ wolves. Their primary goals are to protect and assist the aged and vulnerable. The remaining wolves are omega wolves, who are at the bottom of the order of dominance. Managing the hunting mechanisms is the main goal of the dominance hierarchy of grey wolves. The α wolf orders the β and δ wolves to surround and attack prey once they have located it. The remaining wolves assist in re-enclosing the prey if it were able to get away. Every solution to a suitable optimisation problem in GWO functions similarly to a wolf in a pack. In GWO, the ω wolves represent the remaining candidate solutions, while the first three levels of the dominance hierarchy α, β, δ, and γ represent the optimal, second-optimal, and third-optimal solutions, respectively. Subsequent to formulation (20) must be used to update and enhance solutions that fall within the level

$$d_\omega = |bx_p^{(t)} - x^{(t)}|$$

$$x^{(t+1)} = x_p^{(t)} - ad$$

$$a = 2\mu r_1 - \mu$$

$$b = 2r_2$$

$$\mu = 2 - t\frac{2}{T} \quad (20)$$

where T denotes the maximum number of iterations; b∈Rn and a∈Rn represent coefficient vectors; r1∈Rn and r2∈Rn denote random vectors; and xp(t)∈Rn and x(t)∈Rn represent the prey position and the positions of the entire wolf pack, respectively, at the t-th iteration. GWO employs a values to keep exploration and exploitation in check; method will explore search space if | a | > 1 and exploit the search if 1 a 1. By randomly altering its values, coefficient vector b enhances GWO's search mechanism to prevent stagnation in local optima. Every iteration should update and improve ω level solutions based on top three solutions, which include α, β, and δ. The following formulations are used to carry out this updating mechanism is given by eqn (21)

$$d_\alpha = |b_1 x_\alpha - x|$$

$$d_\beta = |b_2 x_\beta - x|$$

$$d_s = |b_3 x_s - x|,$$

$$x_1 = x_\alpha - a_1 d_\alpha$$

$$x_2 = x_\beta - a_2 d_\beta$$

$$x_3 = x_\delta - a_3 d_\delta$$

$$x(t+1) = \frac{x_1 + x_2 + x_3}{3} \quad (21)$$

where a1, a2, and a3 are calculated, and the first three best solutions are represented by the coefficients xα, xβ, and xδ.

7. RESULTS AND DISCUSSION:

Simulation setup- To justify performance of proposed method for emotion detection using MATLAB software. The system configuration consists of an I7 CPU, 16GB of RAM, and Windows 10 OS. The tool version is R2014a. MATLAB comes with a kernel library and a simple support library file for the existing SVM. On the other hand, a function file defines and programs the classifier's other functions, whereas a library file compiles them. to verify the algorithm's performance using the EEG-based emotion dataset. Model Implementation-For streaming data categorisation performance, a suitable time window length is essential. Wang et al. have discovered that the ideal window length for emotion identification is one second. Therefore, the temporal frame length in this paper is set at 1 s. As the signals were reduced to 128 Hz, the baseline signals prior to the trial were divided into three 32×128 matrices to compute the BaseMean matrix. Trial signal is then subjected to the pre-process operation. After the pre-processing stage, divide the pre-processed EEG signals from each trial's 32 channels into 60 1-second segments using a sliding window. This indicates that 128 is the window size S. Following segmentation, each subject will have a total of 2400 samples (40 trials × 60 segments). After that, the 2D data frames are resized to 9 by 9. Utilise 10-fold cross-validation to assess this method's effectiveness. The final findings of the experiment are determined by averaging the performance of the 10-fold validation procedures.

8. COMPARISON

A confusion matrix used to instrument for summarizing how well a classification algorithm performs. Relying solely on classification accuracy can be deceptive. results when a dataset contains multiple classes or an imbalanced number of samples across classes. Analyzing the confusion matrix provides a clearer understanding of the types of errors produced by the classification model. Although a confusion matrix can be readily extended to multiclass problems by adding corresponding rows and columns, it can also be effectively applied to binary classification tasks. Table 3 shows results of confusion matrix that was used to confirm the accuracy of the data used. For instance, 68% of the cases involving melancholy were correct.

Table 3. Matrix.of Confusion

Category	Normal	Angry	Afraid	Happy	Sad	Total
Normal	66.3	7	6	2.5	18.2	100%
Happy	11.9	10.1	12.5	61.4	4.1	100%
Angry	10.6	72.2	6.3	5.2	5.6	100%
Sad	11.8	4.7	14.3	1	68.3	100%
Afraid	11.8	5.1	49.5	9.4	24.2	100%

Figure 2 presents the confusion matrix employed to assess the classification effectiveness indicators. The matrix includes both the actual and predicted class labels, providing a basis for evaluating the classification results. It helps identify the agreement and discrepancies between the actual and predicted classes. False Positive (FP) denotes the count of negative samples wrongly identified as positive, while False Negative (FN) signifies the count of positive samples mistakenly categorized as negative. True Positive (TP) indicates the count of positive samples accurately identified as positive, whereas True Negative (TN) signifies the count of negative samples accurately identified as negative.



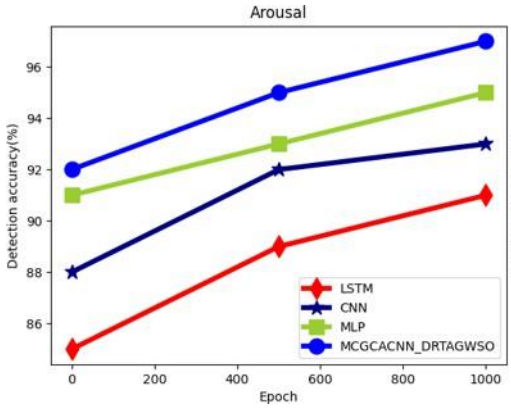
Confusion matrix of DEAP dataset Confusion matrix of SEED dataset

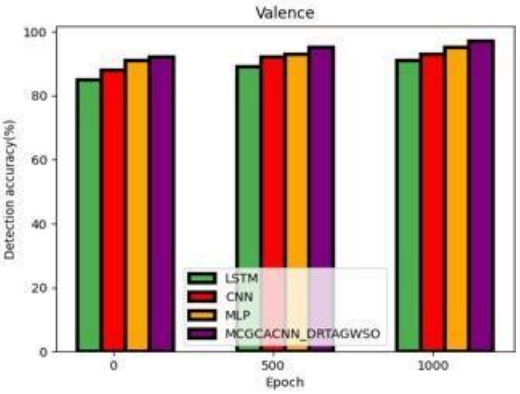


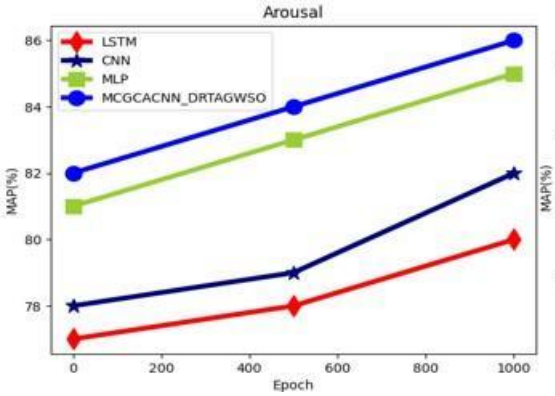
Confusion matrix of GAMEEMO dataset

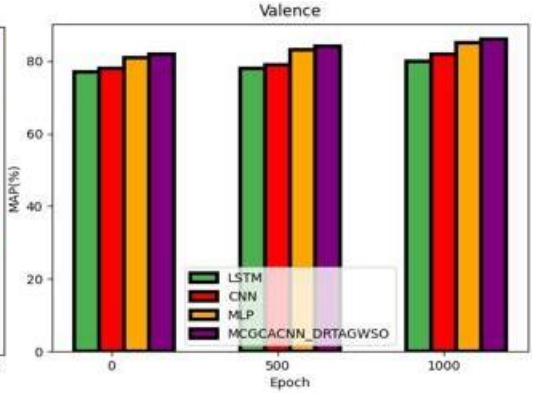
Fig 2: Confusion Matrix for Proposed EEG signal based emotion detection (a) DEAP dataset (b) SEED dataset, (c) GAMEEMO dataset

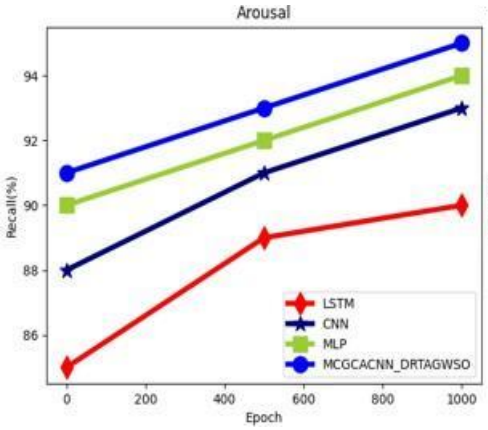
The DEAP dataset is used to evaluate the effectiveness of the suggested network. Ten-fold cross-validation is used to improve the impartiality of experimental outcomes. Figure 3 illustrates the training process of the suggested network on the dataset. Figure 3 (a)–(e) illustrates the training process for the two emotional dimensions of arousal and valence utilizing the DEAP dataset. When the training time on the DEAP dataset is less than 750, both training and validation accuracy rise as the number of epochs increases. Training precision and confirmation duration probably to be steady when epoch is larger than 750. Figure 3 illustrates that the curves corresponding to Positive and negative emotions are located between 0.9 and 1.0, highlighting the enhanced classification effectiveness attained by the suggested approach. Additionally, the confusion matrix (Figure 3) shows that only 18 positive emotion samples and 9 negative emotion samples were misidentified, suggesting that suggested network was highly effective at sorting samples of each class.

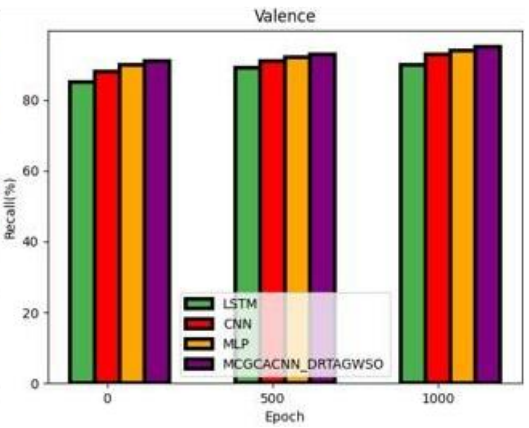

Arousal
Detection accuracy(%)
Epoch
LSTM
CNN
MLP
MCGCACNN_DRTAGWSO


Valence
Detection accuracy(%)
Epoch
LSTM
CNN
MLP
MCGCACNN_DRTAGWSO


Arousal
MAP(%)
Epoch
LSTM
CNN
MLP
MCGCACNN_DRTAGWSO


Valence
MAP(%)
Epoch
LSTM
CNN
MLP
MCGCACNN_DRTAGWSO


Arousal
Recall(%)
Epoch
LSTM
CNN
MLP
MCGCACNN_DRTAGWSO


Valence
Recall(%)
Epoch
LSTM
CNN
MLP
MCGCACNN_DRTAGWSO

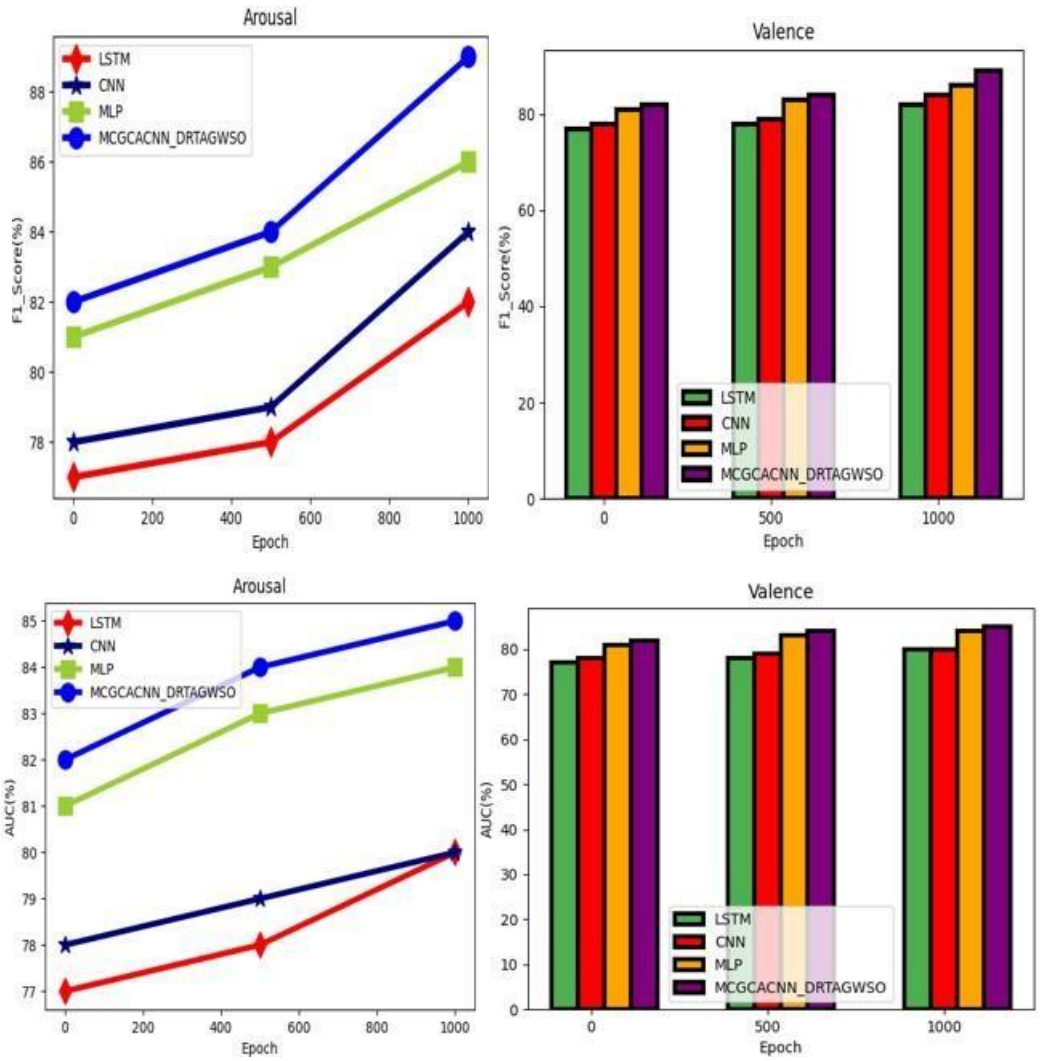


Fig-3 comparative analysis of proposed and existing model for (a) detection accuracy, (b) mean average precision, (c) recall, (d) F-1 score, (e) AUC based on Arousal and valence.

Since 25,600 PCC feature images were generated from The total count of labelled PCC feature images was 25,600 multiplied by four, resulting in 102,400, derived from the primary frequency and three sub-band frequencies. In the course of model development, 90% of the data was designated for training, whereas 5% was reserved for validation and the final 5% for testing. The model assessed its effectiveness on the validation dataset throughout the training phase. Figure 4(a)–(e) presents the accuracy and loss curves for the binary and three-class classification of valence and arousal. It is evident from these graphs that for both procedures, the smallest loss happens between 45 and 50 epochs.Similar to the ML method, which trains the system over 50 epochs, minimising loss is preferable to maximising accuracy.

Table 4 provides the overall classification report that includes the detection accuracy, mean average precision, recall, F-1 score, AUC values for each class of two distinct methods.

Valence/ arousal	Existing technique	Detection accuracy	Mean average precision	Recall	F1_Score	AUC
Protocol 1: 0= low, 1=high						

Valence	**LSTM**	0.74	0.6	0.54	0.61	0.55
	CNN	0.81	0.66	0.56	0.63	0.58
	MLP	0.85	0.68	0.58	0.65	0.61
Arousal	**LSTM**	0.79	0.65	0.59	0.62	0.58
	CNN	0.85	0.68	0.58	0.64	0.61
	MLP	0.88	0.71	0.61	0.68	0.63
Protocol 2: 0= low, 1= medium, 2= high						
Valence	**LSTM**	0.69	0.61	0.59	0.66	0.51
	CNN	0.71	0.63	0.62	0.69	0.55
	MLP	0.73	0.66	0.65	0.72	0.59
Arousal	**LSTM**	0.68	0.65	0.63	0.67	0.62
	CNN	0.73	0.68	0.68	0.69	0.65
	MLP	0.75	0.71	0.73	0.75	0.68

For both protocols, the significance of precision as well as recall was balanced and good, as indicated by the high F1 score. Only the inter-channel correlations were taken into account here. However, inter-sample correlations can be an alternative for further research. It was significant because it made it possible to take into account how temporal features of EEG data varied depending on the emotional state. Furthermore, by increasing the amount of data, inter-sample correlation technique will improve performance of deep ML method for large-scale data. Both lines show a steady growing trend as number of epochs rises. Outstanding performance on training data is shown by training accuracy, which is close to 1.0. Even though the accuracy of validation also increases during training, it eventually stabilizes at approximately 0.8 is a, good but not an optimal performance in the dataset of validation. These results imply that method is successfully gaining knowledge from training set as well as improving its ability to produce precise forecasts. However, if when the validation accuracy levels off or drops after a certain stage while the training accuracy keeps rising, it could suggest overfitting. This implies that the model possesses become excessively tailored to the training data and could have limited generalization ability when applied to new or unseen data. Both training as well as validation losses are shown in the loss map. At first, both metrics show a steep decline, but after around 10 epochs, training loss keeps declining while validation loss begins to rise, suggesting overfitting. This trend indicates that the model is effectively improving. its predictive power by learning from the training data. This study adds to the continuous DL efforts to maximise model performance across a range of datasets. The outcomes are encouraging and provide fresh opportunities for this suggested model's investigation and improvement.

9. CONCLUSION:

This research provides a novel segmentation-based optimization technique designed for recognizing emotions through multi-channel EEG signals and a machine learning model. Emotion identification through multi-channel EEG signals and machine learning involves categorizing emotional states via ML algorithms by analyzing brain activity captured by two EEG channels. Here, the EEG signal is provided as the input and subsequently subjected to normalization and noise reduction. The preprocessed signal is then segmented using a convolutional neural network integrated with multi-channel graph-cut attention. The discrete residual transform and artificial grey wolf swarm optimisation were used to pipeline the segmented EEG input. Each channel subset is represented as a potential solution in the channel selection process, which is phrased as an optimisation problem. The fitness function is the classification accuracy. The findings of the experimental evaluation demonstrated the high performance of the suggested strategy, outperforming other metaheuristics. It could be used in human-computer interaction as well as affective computing, enhancing the emotional intelligence of technology. It is anticipated that future research in the emotion detection field will expand types of test data accessible in order to enhance assessments. Additionally, after gathering EEG data from additional people, self-supervised learning methods may be applied to perhaps create a plug-and-play authentic EEG emotion recognition system. Methods such as the contrastive learning method use unlabelled data to impart information on their own. Enhancing performance utilizing 32-channel EEG devices for emotion recognition is also necessary.

Acknowledgment N/A

REFERENCE:

[1] Wang, Y., Tian, W., Xu, J., Tian, Y., Xu, C., Ma, B., ... & Liu, H. (2023). Wearable wireless dual-channel EEG system for emotion recognition based on machine learning. *IEEE Sensors Journal*, *23*(18), 21767-21775.

[2] Jafari, M., Shoeibi, A., Khodatars, M., Bagherzadeh, S., Shalbaf, A., García, D. L., ... & Acharya, U. R. (2023). Emotion recognition in EEG signals using deep learning methods: A review. *Computers in Biology and Medicine*, *165*, 107450.

[3] Kamble, K. S., & Sengupta, J. (2021). Ensemble machine learning-based affective computing for emotion recognition using dual-decomposed EEG signals. *IEEE Sensors Journal*, *22*(3), 2496-2507.

[4] Saha, O., Mahmud, M. S., Fattah, S. A., & Saquib, M. (2022). Automatic emotion recognition from multi-band EEG data based on a deep learning scheme with effective channel attention. *Ieee Access*, *11*, 2342-2350.

[5] Houssein, E. H., Hammad, A., & Ali, A. A. (2022). Human emotion recognition from EEG-based brain–computer interface using machine learning: a comprehensive review. *Neural Computing and Applications*, *34*(15), 12527-12557.

[6] Liu, H., Lou, T., Zhang, Y., Wu, Y., Xiao, Y., Jensen, C. S., & Zhang, D. (2024). EEG-based multimodal emotion recognition: A machine learning perspective. *IEEE Transactions on Instrumentation and Measurement*.

[7] Dadebayev, D., Goh, W. W., & Tan, E. X. (2022). EEG-based emotion recognition: Review of commercial EEG devices and machine learning techniques. *Journal of King Saud University-Computer and Information Sciences*, *34*(7), 4385-4401.

[8] Samal, P., & Hashmi, M. F. (2024). Role of machine learning and deep learning techniques in EEG-based BCI emotion recognition system: a review. *Artificial Intelligence Review*, *57*(3), 50.

[9] Samavat, A., Khalili, E., Ayati, B., & Ayati, M. (2022). Deep learning model with adaptive regularization for EEG-based emotion recognition using temporal and frequency features. *IEEE Access*, *10*, 24520-24527.

[10] Li, D., Xie, L., Wang, Z., & Yang, H. (2023). Brain emotion perception inspired EEG emotion recognition with deep reinforcement learning. *IEEE Transactions on Neural Networks and Learning Systems*.

[11] Wang, Q., Wang, M., Yang, Y., & Zhang, X. (2022). Multi-modal emotion recognition using EEG and speech signals. *Computers in Biology and Medicine*, *149*, 105907.

[12] Alam, M. S., Jalil, S. Z. A., & Upreti, K. (2022). Analyzing recognition of EEG based human attention and emotion using Machine learning. *Materials Today: Proceedings*, *56*, 3349-3354.

[13] Mutawa, A. M., & Hassouneh, A. (2024). Multimodal Real-Time patient emotion recognition system using facial expressions and brain EEG signals based on Machine learning and Log-Sync methods. *Biomedical Signal Processing and Control*, *91*, 105942.

[14] Kouka, N., Fourati, R., Fdhila, R., Siarry, P., & Alimi, A. M. (2023). EEG channel selection-based binary particle swarm optimization with recurrent convolutional autoencoder for emotion recognition. *Biomedical Signal Processing and Control*, *84*, 104783.

[15] Ramzan, M., & Dawn, S. (2023). Fused CNN-LSTM deep learning emotion recognition model using electroencephalography signals. *International Journal of Neuroscience*, *133*(6), 587-597.

[16] Bagherzadeh, S., Shalbaf, A., Shoeibi, A., Jafari, M., San Tan, R., & Acharya, U. R. (2024). Developing an EEG-based emotion recognition using ensemble deep learning methods and fusion of brain effective connectivity maps. *IEEE Access*.

[17] Rajpoot, A. S., & Panicker, M. R. (2022). Subject independent emotion recognition using EEG signals employing attention driven neural networks. *Biomedical Signal Processing and Control*, *75*, 103547.

[18] Ari, B., Siddique, K., Alçin, Ö. F., Aslan, M., Şengür, A., & Mehmood, R. M. (2022). Wavelet ELM-AE based data augmentation and deep learning for efficient emotion recognition using EEG recordings. *IEEE Access*, *10*, 72171-72181.

[19] Farokhah, L., Sarno, R., & Fatichah, C. (2023). Simplified 2D CNN architecture with channel selection for emotion recognition using EEG spectrogram. *IEEE Access*, *11*, 46330-46343.

[20] Wagh, K. P., & Vasanth, K. (2022). Performance evaluation of multi-channel electroencephalogram signal (EEG) based time frequency analysis for human emotion recognition. *Biomedical Signal Processing and Control*, *78*, 103966.

[21] Vempati, R., & Sharma, L. D. (2023). A systematic review on automated human emotion recognition using electroencephalogram signals and artificial intelligence. *Results inEngineering*, *18*, 101027.